Strain Response of a Wind Turbine Tower as a Function of Nacelle Orientation

Jeff Bas[1], Rupp Carriveau[2], and Shaohong Cheng[3]
Department of Civil and Environmental Engineering
University of Windsor
Windsor, Ontario, Canada
e. [1]basj@uwindsor.ca, [2]rupp@uwindsor.ca, [3]shaohong@uwindsor.ca

Tim Newson
Department of Civil and Environmental Engineering
University of Western Ontario
London, Ontario, Canada
e. tnewson2@uwo.ca

***Abstract*— A land based 2.3 MW horizontal axis wind turbine steel supporting tower was instrumented with a Fiber Braggs Grating Strain array. The turbine was subjected to forced yawing of the nacelle during periods of low wind in order to isolate a baseline structural response. The strain experienced in the tower was presented as a function of yaw angle, and was shown to vary in a sinusoidal manner as a response to the eccentric loading condition present at the nacelle-tower interface. The yaw-strain baseline was shown to have strong inter-sensor cross correlation and is discussed in the context of a healthy structural response record with possible future utilization in SHM schemes.**

Keywords - Wind Energy; SHM; Strain Response; Wind Turbine Tower

I. INTRODUCTION

Due to the high initial implementation costs of wind energy, increasing the longevity of the entire turbine system is an important factor contributing to the economic viability of wind energy projects [1]. One of the main components of a horizontal axis wind turbine system is the structure's supporting tower. The towers themselves are usually constructed from steel, are assembled in multiple sections [2-4], and are commonly designed to have a lifespan of 20 to 30 years [3-4].

Figure 1: The subject wind turbine located in Southern Ontario, Canada.

Unlike most of the mechanical systems (rotors, control motors, bearings etc.) that can be replaced without dismantling major components of the system, repairing a damaged tower can be a costly procedure requiring specialty surface preparations, welding techniques and surface finishing [4]. In situations where damage is irreparable, replacing a damaged tower section involves an extraordinary amount of down time and resources to complete. In order to replace a full tower section, the entire nacelle and rotor assembly must be disassembled and subsequently re-assembled [5]. The ability to monitor and identify problems within the tower structure in a timely manner could help prevent a small tower defect from growing into a larger problem. This is commonly referred to as structural health monitoring (SHM).

Structural health monitoring has a history of implementation on large scale civil infrastructure such as bridges, dams and pipelines in order to prevent or predict catastrophic structural failure [6]. SHM has also been applied to wind turbine mechanical systems such as rotor and blade assemblies [7-9]. There has recently been interest in the literature regarding SHM of the supporting towers for wind turbines [10-11]. The basic premise of SHM techniques is that damage to a structure, such as a crack in the material, results in the changing of the structures dynamic properties (stiffness, damping, etc.). This change in physical properties results in a change in the structures' response (strain, natural frequencies, mode shape etc.) to service conditions. SHM strategies work to identify the changes in structural response in order to detect structural damage [10, 12-13]. Works examining the response of turbine towers have mostly focused on the structural dynamic response of wind turbine towers by means of finite element analysis [3, 14-18] and in-situ monitoring of wind turbine towers using accelerometers and/or strain gauges [19-21]. The main focus of these studies has been improving tower design methods.

Since many SHM schemes compare measured structural response to that of a typical undamaged or healthy structure, it is necessary to collect a library of response samples corresponding to a healthy state [10, 12-13, 22]. This paper presents longitudinal strain data gathered from a 2.3 MW commercial horizontal axis wind turbine tower in order to further facilitate the characterization of a healthy wind turbine tower response to changes in the nacelle's yaw

 ISBN: 978-1-61208-191-5

positioning. The turbine was subjected to manually forced yawing of the nacelle during low wind conditions. The data was measured by a Fiber Bragg Grating strain sensor array with the ability to detect both static and dynamic tower response. The strain data is presented as a function of yaw angle and is potentially useful as a healthy baseline as a wind turbine with active yaw control is constantly changing its yaw angle in order to be facing the wind. Future possible applications of the sensor array are subsequently discussed.

II. INSTRUMENTATION

The wind turbine tower studied is 78.54 m tall. It was designed for wind gusts of 59.5 m/s with 18% turbulence. It is comprised of three individual steel sections that are bolted together, the geometry of the sections varies throughout the height of the tower. The bottom section is 15660mm tall with a constant outside diameter of 4200mm and wall thicknesses varies from 41mm to 25mm; the middle section of the tower is 26880mm tall with a constant outside diameter of 4200mm and varying wall thicknesses of 24mm to 14mm; the top section of the tower is 36000mm tall with an outside diameter that varies linearly from 4200mm at the base of the section to 2392mm at the top and wall thicknesses varying from 13mm to 22mm. The tower geometry is such that the area moment of inertia decreases as the height of the tower increases, the moment of inertia of the tower with respect to its height is shown in Figure 2. The large moment of inertia at the base is required to counteract the large bending moment induced at the fixed foundation by the wind design loads [3]. The studied tower was also recently subjected to a comprehensive structural inspection and was determined to be in good condition.

The tower was outfitted with a Fiber Bragg Grating (FBG) sensor array. An FBG array was chosen over a traditional foil gauge set up for a number of reasons

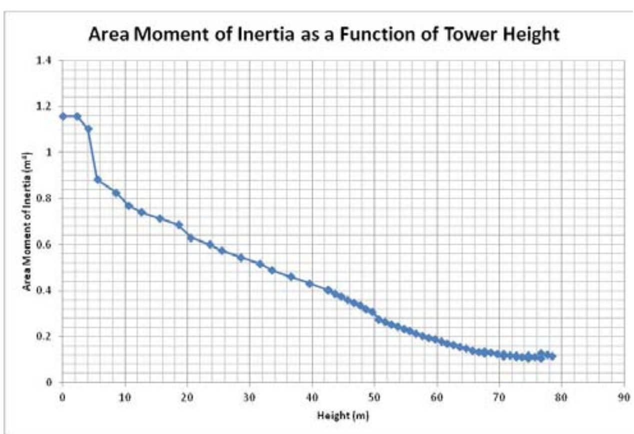

Figure 2:Area moment of inertia of the wind turbine tower as a function of the tower height

including but not limited to; their immunity to electromagnetic interference that may be present during regular operation of the wind turbine [11, 23]. Their corrosion resistance and long service life contributes to their ability to operate for extended periods of time in a variety of harsh conditions such as those experienced by offshore wind turbines in the North Atlantic [6, 11, 23]. Their non conductive nature [23] was of particular importance for this installation given turbine susceptibility to lightning strikes; a 2002 report published by the National Renewable Energy Laboratory found that up to 8% of wind turbines could be expected to experience a lightning strike each year [24]. Strain gauges also have an advantage in measuring static deformations that occur over a long period of time that may otherwise be missed by accelerometers, and are still capable of tracking dynamic responses [6, 9, 11, 23].

The FBG array consisted of two os7100 three dimensional accelerometers, 12 os4100 temperature sensors and 24 longitudinally mounted os3100 strain gauges with a strain sensitivity of 1.4 pm/με, feeding into a sm130 optical sensing interrogator all manufactured by Micron Optics. The strain gauges, and temperature gauges were affixed to the interior of the circular tower by means of an epoxy adhesive at six different heights above the foundation along the tower's vertical axis, shown in Table 1. The vertical location of each of the strain gauge rings were chosen for practical installation with respect to the safety

TABLE I. HEIGHTS ABOVE FOUNDATION

Level	Vertical Height (m)
5	77.34
4	65.02
3	41.84
2	14.46
1	4.46
0	0

landings located throughout the tower. At each level four strain gauges and two temperature gauges were positioned as depicted by Figure 3, with one strain gauge and one temperature sensor at both the 12 o'clock and 6 o'clock position, along with two strain gauges located at the 3 and 9 o'clock positions of the tower respectively. The 12'oclock position corresponds to the true north face of the tower. One accelerometer was placed at level 5 and another was placed at level 3.

As a broadband light source is transmitted through fiber optic cables attached to each strain and temperature gauge, each gauge reflects its own distinct wavelength of light known as the Bragg wavelength λ_B, given by equation 1 below;

$$\lambda_B = 2n\Lambda \qquad (1)$$

 ISBN: 978-1-61208-191-5

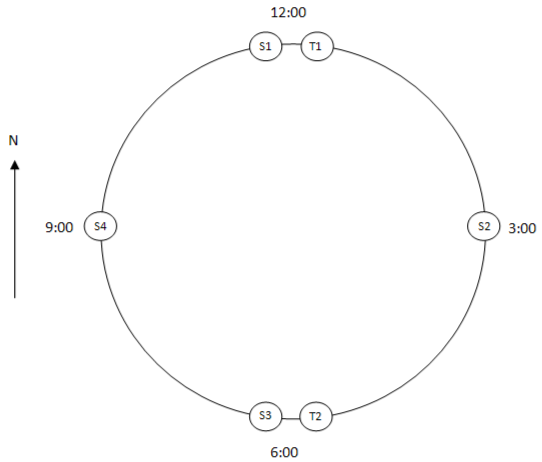

Figure 3: Typical sensor orientation

where n is the effective core index of refraction and Λ the grating period [25]. When a Bragg grating is strained, the grating period shifts, the wavelength strain relationship for a FBG strain gauge is given by Equation 2 below

$$\varepsilon = (10^6)\frac{\Delta\lambda/\lambda_o}{F_G} \tag{2}$$

where ε is the mechanically induced strain, Δλ is the shift in measured wavelength, λ_o is the initial reference wavelength and F_G is a gauge factor which is a property associated with a particular strain gauge that relates the strain measured to the shift in reflected wavelength. It should be noted that the strain gauges are self-referencing. Thus, the strain measured is the change in strain with respect to the original strain reading at the beginning of each experimental recording.

III. EXPERIMENTS

In order to determine a baseline of the relationship between the directional orientations of the nacelle (yaw position) and the strain in the tower at the various strain gauge locations, an experiment was performed on three separate occasions when the wind farm was experiencing periods of low wind, when the wind speeds were lower than the turbines cut-in wind speed of 3 m/s. Low wind periods were chosen for two reasons. First, as the test machine is part of a commercial wind farm, parking a power producing turbine during high yield winds represents financial loss. The second reason was to minimize the proportion of strain response that could be attributed to the wind load. The average wind speeds for each individual experiment are given in Table 2.

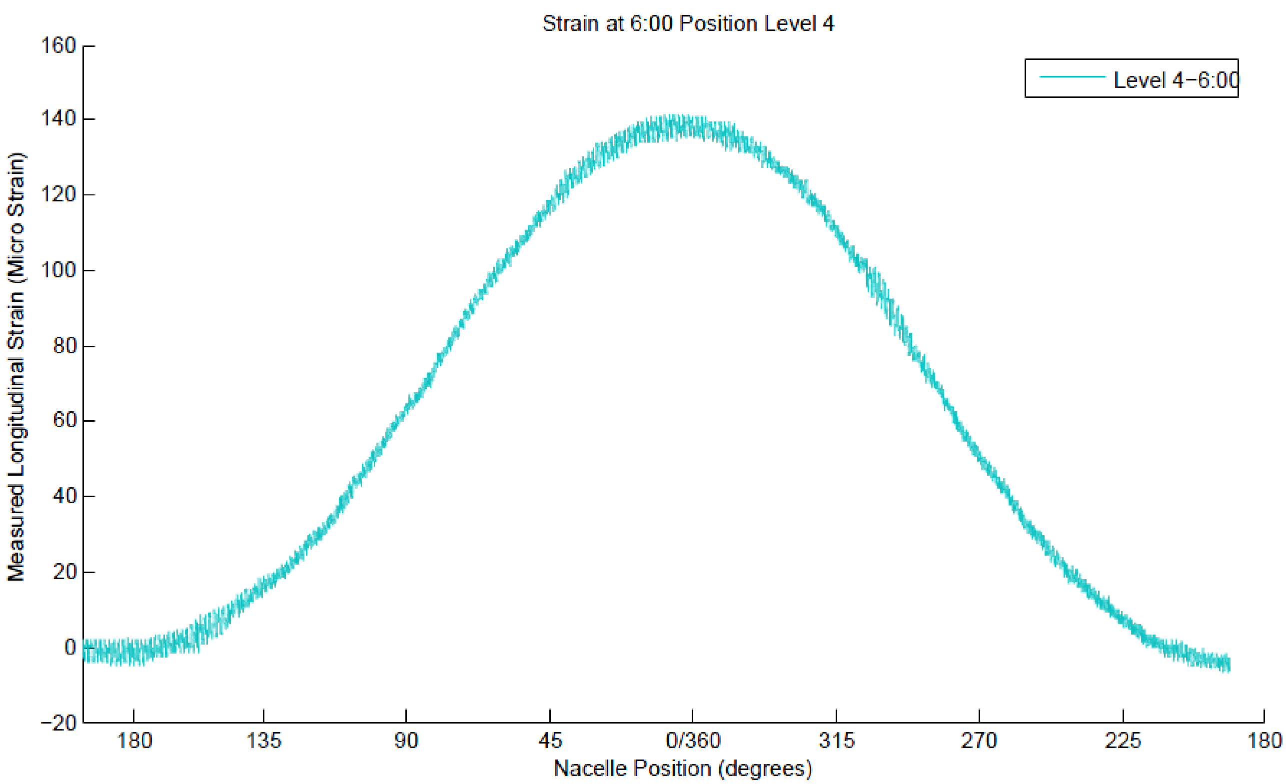

Figure 4: Representative strain-yaw position relationship measured at the strain gauge located on level 4 at the 6:00 position in the tower

TABLE II. AVERAGE WINDSPEEDS DURING EACH INDIVIDUAL EXPERIMENT

Experiment	Average Wind Speed (m/s)
1	2.1
2	1.5
3	2.5

Each experiment consisted of manually yawing the nacelle, using the tower's handheld control module, for three full 360 degree rotations; each rotation took 800 seconds to complete and was performed in the opposite direction of the previous rotations. The opposing rotation directions were necessary due to the limit of the number of rotations the nacelle can complete in one direction without twisting the cables past their maximum limit. Operational constraints built into the tower's control software also required for the rotor brake to be disengaged while the nacelle was put through the rotations. The blades, however, were pitched into a full aerodynamic brake position to ensure minimal rotor motion during the tests.

Strain information was collected via a PC located at the first safety landing platform inside the tower, running Micron Optics' EN-Light data acquisition software. The sampling rate for the Fiber Braggs Grating array was 100 Hz. The general turbine parameters were recorded on a separate PC located at the wind farm's operations office by means of an SQL script with a data sampling rate of 0.2 Hz. The parameters recorded from the turbine were: nacelle yaw position, wind speed, rotor speed, power production and blade pitch. Before the tests, the two data acquisition systems were set to collect data synchronously with a common timestamp.

IV. RESULTS

The resulting strain-yaw position relationships clearly demonstrate the effect of the eccentric load transferred to the turbines' supporting tower induced by the front-heavy nacelle. This is revealed through inspection of the strain-yaw relationship of any strain gauge in the tower. Figure 4 is representative of a typical nacelle rotation and shows the strain-yaw angle relationship of a strain gauge located at a height of 65.02m above the foundation, situated at the 6:00 position of the tower. As the rotor passes over the gauge (yaw angle of 180 degrees), the tower wall experiences an increase in compressive strain. Similarly, an equivalent tensile strain is experienced when the nacelle is oriented above the opposite side of the tower (yaw angle of 0 degrees), resulting in a predictable sinusoidal pattern in the strain-yaw relationship. Every grouping of strain gauges at each measured tower level between level 0 and level 4 inclusive show a similar sinusoidal response pattern. The difference in strain magnitude from peak to peak for each gauge location shows good agreement with its neighboring gauges as shown in Figure 5. The constancy of the strain response at each level indicates that all strain gauges are functioning properly. The strain peaks for each strain gauge along the rotation of the nacelle occur predictably at a ¼ rotation from the previous peak at 0, 90, 180 and 270 degrees. For the result illustrated here, the nacelle rotated in the counter clockwise direction starting from a yaw position of 194 degrees. The duration of the rotation was 13 minutes and 10 seconds and the mean wind speeds observed at nacelle mounted anemometer was 2.5 m/s.

In order to represent the effect of the tower geometry on the magnitude of strain response induced by the eccentric load at the nacelle, we consider all of the strain gauges positioned on the same face of the tower, e.g., the 6 o'clock position as per Figure 6 below. The tower is constructed such that as the height of the tower increases, the area moment of inertia of the tower decreases. Equation (3) represents the contribution of an eccentric load to the strain induced in a column, where; M is the internal moment induced by the loading eccentricity on the column, y is the distance of the point of interrogation from the neutral axis of the column, E is the elastic modulus of the material, and I the moment of inertia of the column.

$$\varepsilon = \frac{My}{EI} \tag{3}$$

Equation 3 indicates that the strain in the tower is inversely proportional to the area moment of inertia of the tower. This is responsible for the large differences in strain measured along the tower's height as demonstrated in Figure 6. The cross correlation coefficients between every strain gauge along the vertical lines for the bottom 5 interrogated levels of the turbine tower was calculated to range between 0.83 and 0.98, showing good correlation throughout the strain array. This strong and consistent inter-sensor correlation may be applicable to detecting damages within the tower structure by means of a correlation-based damage identification method like that described by Gul [22].

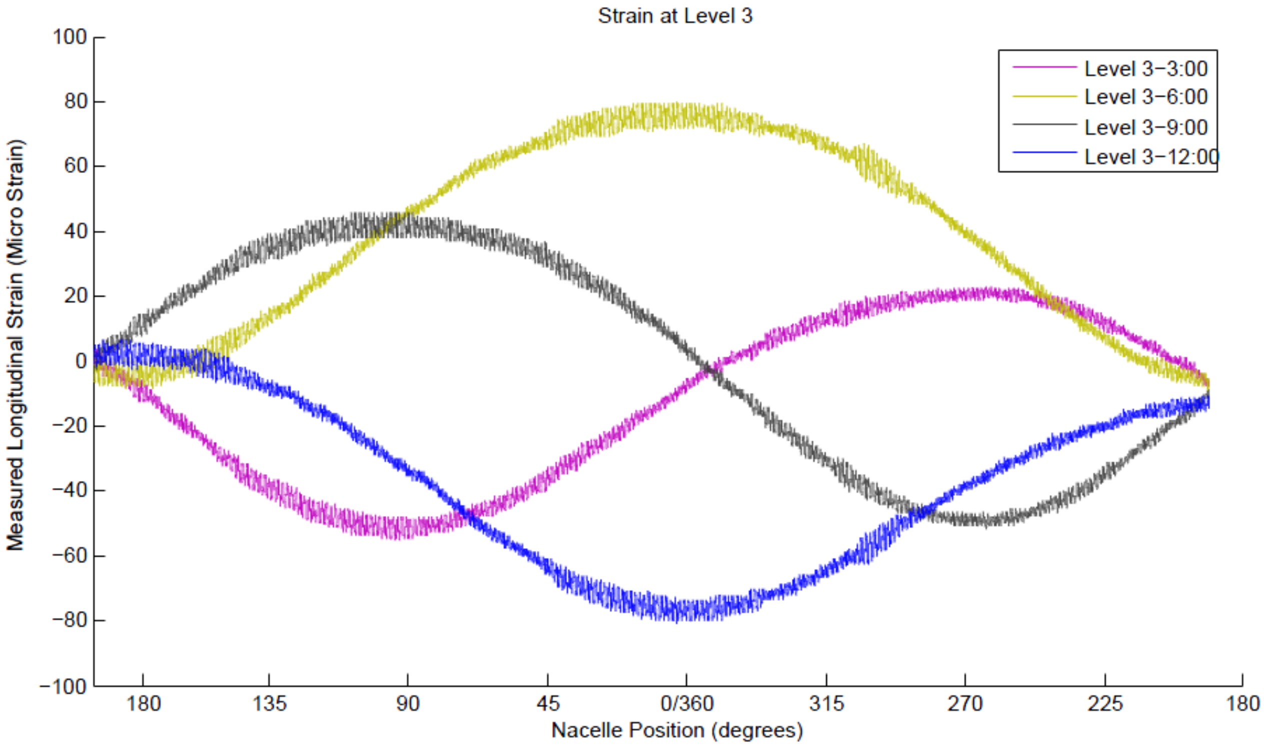

Figure 5: Strain-yaw position relationship measured at Level 3 of the tower.

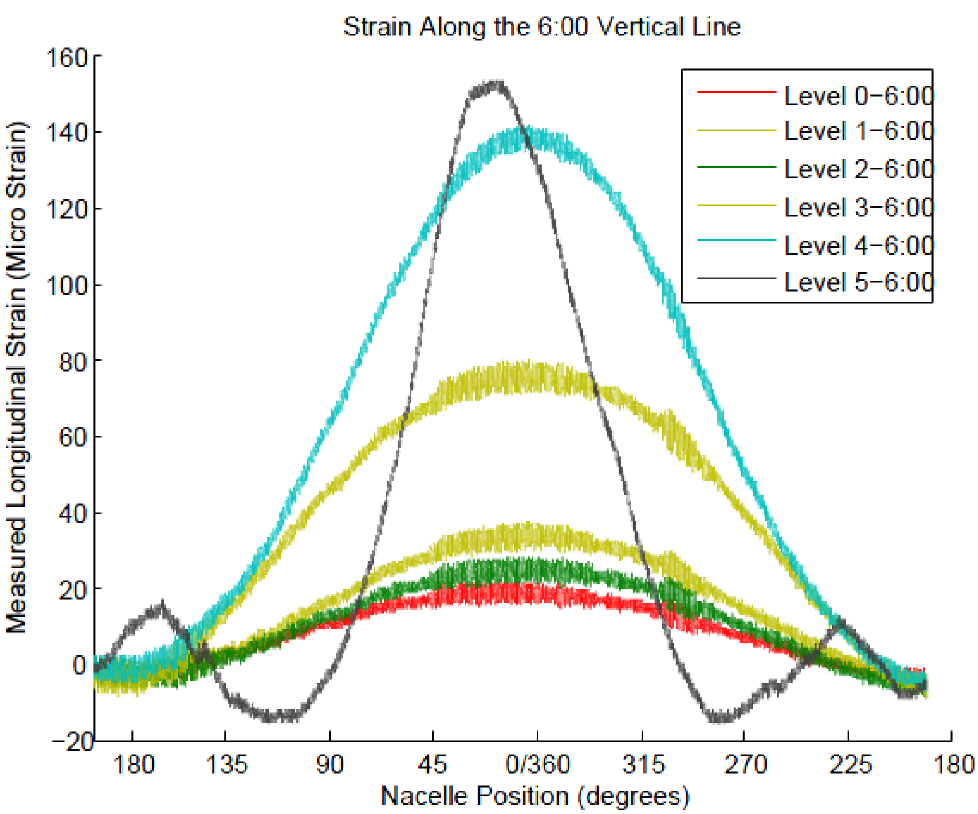

Figure 6: Strain-yaw relationship measured by the strain gauges on the South face of the tower

The difference in strain at 77.34m above the foundation, or the very top ring of strain gauges on level 5, presented in Figure 7, did not behave similarly to all of the other rings below it; rather, each show a large area of peak compression within a yaw range of 90 degrees to the left and right of the nacelle current position. It has been theorized that this was a result of the close proximity of the strain gauges to the nacelle load bearing surface, and the possibility of an imperfectly distributed load over the connecting flange transferring a quasi-point load to the left and right of the turbine rotor.

Since yawing events occur constantly throughout turbine operation, the data sets collected and presented can potentially serve as a baseline to which a future SHM program could compare monitored responses. The strong and consistent inter-sensor correlation may be applicable detecting damages within the tower structure by means of correlation based damage identification methods [22]. This set of raw data will be further analyzed in order to identify healthy dynamic response natural frequencies, modal damping, and mode shapes that can be applied to vibration based SHM schemes.

V. Concluding Remarks and Future Work

The structure and instrumentation of a 2.3 MW horizontal axis wind turbine tower using an FBG strain array was described. Three separate experiments held on three different low wind days, investigated the strain response of the supporting tower induced by yawing the nacelle a full 360 degrees. The following can be concluded from the results presented:

- It was identified that the nacelle yaw position-strain relationship demonstrated the presence of an eccentric load transferred to the tower from the nacelle.
- There is the presence of a strong cross correlation between each of the individual responses from the bottom 5 strain gauges oriented along the same vertical line. This correlation could be used as the baseline tower behavior for a correlation-based damage identification method.
- There was a consistent and recurring anomaly in the strain response of the 4 individual strain gauges located at the top level of the tower. It is theorized that the anomaly is a result of stress concentrations at the tower-nacelle interface due to an unequally distributed load.

Moving forward with the results and capabilities of the configured system; the following is being considered: A characterization of the structural response of the tower to different types of rotor braking events. The potential for accelerated fatigue damage promoted through soft, hard, and emergency stops will be studied. Another future work will be focused on the correlation of the tower response due to operational loading measured by means of the SCADA system, a meteorological tower in close proximity to the tower as well as a nacelle mounted LIDAR unit. Finally the system will continually contribute to the development of a

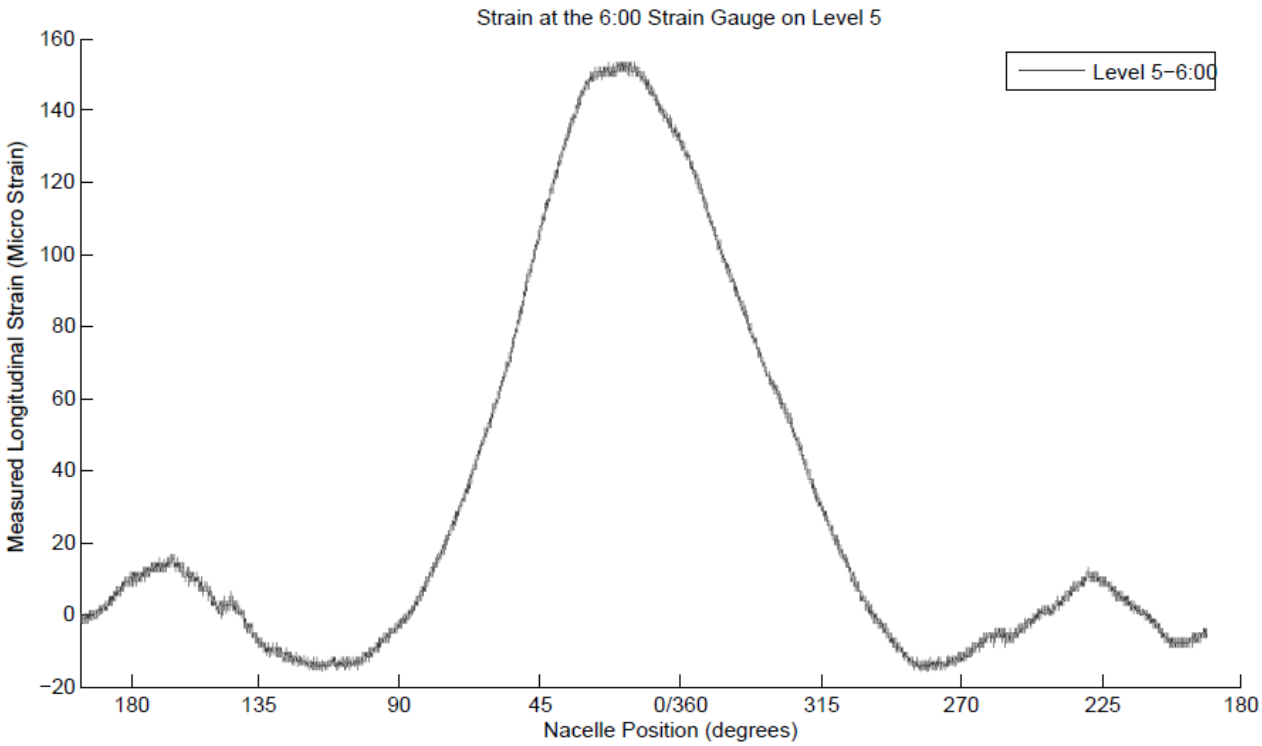

Figure 7: Representative strain-yaw position relationship measured at the strain gauge located on level 5 at the 6:00 position in the tower

database of the healthy structural tower signatures during regular operating conditions.

REFERENCES

[1] M. Kenisarin, “Worldwide state of wind-power engineering,” Applied Solar Energy, vol. 38, 2002, pp. 73-87.

[2] G. Horvath and L. Toth, “New methods in wind turbine tower design,”. Wind Engineering, vol. 25, 2001, pp. 171-178, doi:10.1260/0309524011495971.

[3] I. Lavassas, P. Zervas, E. Efthimiou, I.N. Doudoumis and C.C. Baniotopoulos, “Analysis and design of the prototype of a steel 1-MW wind turbine tower,” Engineering Structures,vol. 25, July 2003, pp. 1097-1106, doi: 10.1016/S0141-0296(03)00059-2.

[4] A. Nestor, “Defects, damages, and repairs subject to high cycle fatigue: Examples from wind farm tower design,” 5th Congress on Forensic Engineering, 2009, pp. 546-555.

[5] R. Lacalle, S. Cicero, J. Álvarez, R. Cicero and V. Madrazo, “On the analysis of the causes of cracking in a wind tower,” Engineering Failure Analysis, vol. 18, Oct. 2011, pp. 1698–1710, doi:10.1016/j.engfailanal.2011.02.012.

[6] M. Feng, “Application of structural health monitoring in civil infrastructure,” Smart Structures and Systems, vol. 5, July 2009, pp. 469-482.

[7] J. White and D. Adams, “Experimental results of wind turbine operational monitoring with structural and aerodynamic measurements,” 29th IMAC, a Conference on Structural Dynamics, vol. 5, Jan. 2011, pp. 325-331.

[8] H.J. Sutherland, N.D. Kelley and M.M. Hand, “Inflow & fatigue response of the NWTC advanced research turbine,” ASME 2003 Wind Energy Symposium, WIND2003, Jan. 2003, pp. 214-224.

[9] M. Volanthen, “Fibre optic strain measurement for aerospace structures - Lessons from their use in the offshore oil and gas, and wind energy industries,” 4th European Workshop on Structural Health Monitoring, July 2008, pp. 855-862.

[10] K. Bassett, R. Carriveau and D. S-K. Ting, “Vibration response of a 2.3 MW wind turbine to yaw motion and shut down events,” Wind Energy, vol. 14, Feb. 2011, pp. 939–952, doi:10.1002/we.457

[11] H. Bang, M. Jang and H. Shin, “Structural health monitoring of wind turbines using fiber Bragg grating based sensing system,” Sensors and Smart Structures Technologies for Civil, Mechanical, and Aerospace Systems 2011, vol. 7981, Mar. 2011, pp. 1-8, doi:10.1117/12.880654.

[12] L. Card and D.K. McNeill, “Characterization of system sensitivity in SHM event-detection systems,” Nondestructive Evaluation and Health Monitoring of Aerospace Materials, Composites, and Civil Infrastructure IV, vol. 5767, Mar. 2005, pp. 143-154, doi:10.1117/12.599944.

[13] W. Fan, P. Qiao, “Vibration-based Damage Identification Methods: A Review and Comparative Study,” Structural Health Monitoring, vol 10, Jan. 2011, pp. 83-111, doi:10.1177/1475921710365419

[14] W. Lai and D. Xitong, “Influence of earthquake directions on wind turbine tower under seismic action,” 1st International Conference on Civil Engineering, Architecture and Building Materials, CEABM 2011. Vol. 243-249, June 2011, pp. 3883-3888, doi: 10.4028/www.scientific.net/AMR.243-249.3883

[15] B. Luong Van, I. Takeshi, P. Pham Van and Y. Fujino, “A peak factor for non-Gaussian response analysis of wind turbine tower,” Journal of Wind Engineering and Industrial Aerodynamics, vol. 96, Oct. 2008, pp. 2217-2227, doi:10.1016/j.jweia.2008.02.019.

[16] P.J Murtagh, B. Basu and B.M. Broderick, “Along-wind response of a wind turbine tower with blade coupling subjected to rotationally sampled wind loading,” Engineering Structures, vol. 27, July 2005, pp. 1209-1219, doi:10.1016/j.engstruct.2005.03.004.

[17] X. Chen, J. Li and J. Chen, “Wind-induced response analysis of a wind turbine tower including the blade-tower coupling effect,” Journal of Zhejiang University SCIENCE A, vol 10, Nov. 2009, pp. 1573-1580, doi:10.1631/jzus.A0820750.

[18] Y. Xu, S. Wenlei and Z. Jianping, “Static and dynamic analysis of wind turbine tower structure” 7th International Conference on Fracture and Strength of Solids, FEOFS 2007, vol. 33-37 part 2, 2008, pp. 1169-1174.

[19] M. Molinari, M. Pozzi, D. Zonta and L. Battisti1, "In-field testing of a steel wind turbine tower,” 28th IMAC, A Conference on Structural Dynamics, 2010, vol. 1, 2011, pp. 103-112.

[20] R.A. Swartz, J.P. Lynch, S. Zerbst, B. Sweetman and R. Rolfes, “Structural monitoring of wind turbines using wireless sensor networks” Smart Structures and Systems, vol. 6, Apr. 2010, pp. 183-196.

[21] M.C. Pollino and A.A. Jr. Huckelbridge, “Initial observations from monitoring the in-situ performance of a community-scale wind turbine support structure,” 2011 IEEE Energytech, May 2011, pp. 1-4, doi:10.1109/EnergyTech.2011.5948540.

[22] M. Gul, H.B. Gokce and F.N. Catbas, “A characterization of traffic and temperature induced strains acquired using a bridge monitoring system,” Structures Congress 2011, 2011, pp. 89-100, doi:10.1061/41171(401)9

[23] T. Graver, “What are the specific advantages of FBG sensors?”, Micron Optics Blog, June 2008.

[24] B. McNiff, “Wind Turbine Lightning Protection Project 1999-2001,” E. Muljadi, Editor. 2002, National Renewable Energy Laboratory: Harborside, Maine.

[25] Y.J. Rao, “In-Fiber Bragg grating sensors,” Measurement Science and Technology, vol. 8, 1997, pp. 355-375.